Mouse model of chorea-acanthocytosis exhibits male infertility caused by impaired sperm motility as a result of ultrastructural morphological abnormalities in the mitochondrial sheath in the sperm midpiece

Omi Nagata[1], Masayuki Nakamura[1]*, Hitoshi Sakimoto[1], Yuka Urata[1], Natsuki Sasaki[1], Nari Shiokawa[1], Akira Sano[1]

[1.] Department of Psychiatry, Kagoshima University Graduate School of Medical and Dental Sciences, 8-35-1 Sakuragaoka, Kagoshima 890-8520, Japan

*Corresponding author: Masayuki Nakamura, Department of Psychiatry, Kagoshima University Graduate School of Medical and Dental Sciences, 8-35-1 Sakuragaoka, Kagoshima 890-8520, Japan .

Tel.: +81-99-2755346; Fax: +81-99-2657089

E-mail address: nakamu36@m.kufm.kagoshima-u.ac.jp

Abstract

Chorea-acanthocytosis (ChAc) is an autosomal recessive hereditary disease characterized by neurodegeneration in the striatum and acanthocytosis caused by loss-of-function mutations in the Vacuolar Protein Sorting 13 Homolog A (*VPS13A*) gene, which encodes chorein. We previously produced a ChAc-model mouse with a homozygous deletion of exons 60–61 in *Vps13a*, which corresponded to the human disease mutation. We found that male ChAc-model mice exhibited complete infertility as a result of severely diminished sperm motility. Immunocytochemical study revealed that chorein-like immunoreactivity is abundant only in the midpiece, mitochondria-rich region, of the sperm of wild type mice. They showed no significant differences from wild types in terms of the adenosine 5′-triphosphate (ATP) concentration of their sperm, sperm count, or sexual activity. Electron microscopy revealed abnormal ultrastructural morphology of the mitochondria in the midpiece of sperm from ChAc-model mice. These results suggest that chorein is essential in mouse sperm for the maintenance of ultrastructural mitochondrial morphology and sperm motility.

Key words

Chorea-acanthocytosis; ChAc-model mouse; male infertility; asthenozoospermia; *Vps13a*; chorein; mitochondria

Abbreviations

ChAc, chorea-acanthocytosis; *VPS13A*, Vacuolar Protein Sorting 13 Homolog A; PBS, phosphate-buffered saline; ATP, Adenosine 5′-triphosphate

Introduction

In humans, loss-of-function mutations in the Vacuolar Protein Sorting 13 Homolog A (*VPS13A*) gene, which encodes a large protein named chorein, causes chorea-acanthocytosis (ChAc; MIM 200150) [1–4], an autosomal recessive neurodegenerative disorder. Clinically, ChAc is characterized by adult-onset chorea, acanthocytosis in erythrocytes, and Huntington's disease-like neuropsychiatric symptoms. The main neuropathological feature of ChAc is the neurodegeneration of the striatum.

We produced a ChAc-model mouse with a hybrid genetic background (129/sv and C57BL/6J) by deleting exons 60–61 of *Vps13a*, which mimics the human disease mutation [5]. ChAc-model mice that were backcrossed with different inbred strains exhibited differences in symptoms [6]. While conducting these experiments, we found male infertility in ChAc-model mice carrying homozygous exon 60–61 deletions in *Vps13a* [7]. While we experienced human male ChAc patients with normal reproductive capacity, there is one case report of male infertility in a patient with neuroacanthocytosis [8]. Recently, Kevin Peikert et al. reported two male ChAc patients with infertility due to asthenoteratozoospermia and oligoasthenozoospermia,

respectively in the ninth International Meeting on Neuroacanthocytosis Syndromes. The abstract of this study in the meeting is in press in Tremor and Other Hyperkinetic Movements.

In the present study, we confirmed male infertility in ChAc-model mice and performed assessment tests for sexual activity and sperm condition, together with an electron-microscopy analysis of sperm morphology, to identify the causes of male infertility in ChAc-model mice.

2. Materials and methods

2.1. Animals

ChAc-model mice (*Vps13a*^{tm1asan} mice) with a homozygous deletion of exons 60–61 in *Vps13a*, corresponding to a human disease mutation, were produced by gene targeting as previously described [5,9]. We primarily used an inbred strain 129S6/SvEv (wild type) (Taconic Labs, Hudson, NY, USA), and strain 129S6/SvEv-*Vps13a*^{tm1asan} (ChAc$^{Del/Del}$), which we produced previously [6]. This study was carried out in accordance with the guidelines for Animal Experimentation (MD14017) and Gene

Recombination Experiments (24054) of the Graduate School of Medical and Dental Sciences, Kagoshima University, Japan. Mice were group-housed with normal light–dark cycles (lights on at 7:00 AM, lights off at 7:00 PM) in a clean facility, and were given free access to food and water.

2.2. Infertility test

Each of four male $ChAc^{Del/Del}$ mice were mated with female wild-types for 19.5 ± 5.2 (15 to 24) weeks. Each of five female $ChAc^{Del/Del}$ mice was also mated with male wild-types for 5.4 ± 2.9 (3 to 9) weeks.

2.3. Odor-sniffing test

The odor sniffing test was performed as described by Kobayakawa et al. [10] with minor modifications. Mice (n = 8 wild-type; n = 7 $ChAc^{Del/Del}$) were habituated to the cage, after which a cotton swab soaked with distilled water was presented for 3 min. This was repeated three times at 1-min intervals. Then a cotton swab soaked with the indicated amount of the test odorants (first female urine and then male urine) was

presented in the same way. Mouse behavior was recorded with a digital video camera (1440 × 1080 pixels) for analysis. We defined 'an investigation' as nasal contact within 1 mm of the cotton swab, and we measured the duration of each investigation.

2.4. Male sexual behavior test

The male sexual behavior test was performed as described by Haga et al. [11], with minor modifications. Each of the male mice (n = 6 wild-type; n = 6 $ChAc^{Del/Del}$) was individually housed in a test cage 24 hours before the test. After 24 hours, the mice were paired with a sexually naive female wild-type mouse and their behavior was video-recorded (1440 × 1080 pixels) for 1 h during the dark phase under a 50-lux light. The total number of male mounting behaviors was scored.

2.5. Sperm collection, count, and motility

Epididymides from wild-type and $ChAc^{Del/Del}$ mice were dissected, and then the cauda regions were separated. Immediately, multiple incisions were made in the tissue, and sperm from each tissue were gently scraped out or allowed to swim into 1 ml of warmed

saline. The sperm solution was loaded into the hemocytometer chamber. After assessing samples for 10–15 minutes, at least 200 sperm were counted per replicate (n = 3 wild-type; n = 3 $ChAc^{Del/Del}$). Then the concentration of sperm per region was calculated. Microscopic observation video recordings were made of three randomly selected regions (n =10 wild-type; n =10 $ChAc^{Del/Del}$). Under light-microscope observation, the number of sperm displaying abnormal morphology, classified according to World Health Organization (WHO) guidelines [12], was also blindly calculated. The motility of all sperm within a defined area of the field was assessed according to WHO categories of sperm movement [12]. First, the grid section being scored for progressive motility (PR) cells was scanned. Next, non-progressive motility (NP) sperm, and finally immotile (IM) sperm, were counted in the same grid section. The total number of sperm that were classified as either NP or IM was calculated as the "motility-failure rate".

2.6. Immunocytochemical study

To prepare the discontinuous Percoll (Sigma) density gradient, Percoll solution was diluted with phosphate-buffered saline (PBS) to make 20–80% Percoll solutions at

graduated intervals of 20%. The epididymides from wild-type mice were dissected, then the cauda regions were separated. Immediately, multiple incisions were made in the tissue, which was placed into 0.3 ml of PBS and incubated for 1 h. After removing the epididymis, the 0.3-ml sperm suspension was placed at the top of the Percoll density-gradient column and centrifuged at 400 × g for 20 min. The bottom fraction was washed twice with 1 ml PBS. The supernatant was removed and 375 μl of 400 nM MitoTracker Green FM (Invitrogen) with PBS was added. Sperm stained with MitoTracker Green FM were washed three times with PBS. Subsequently, sperm were fixed for 15 min in 0.1 M phosphate buffer containing 4% (w/v) paraformaldehyde. The fixed sperm were washed three times with PBS–Glycine (0.01 M glycine in PBS, pH 7.4), then permeabilized with PBS containing 0.1% (w/v) Triton X-100 for 5 min. Sperm were then washed three times with PBS–Glycine and blocked for 1 h at room temperature with 10% (w/v) non-fat dried milk in PBS containing 0.1% (w/v) tween 20 and 6% (w/v) glycine (PBS-T). Sperm were incubated with rabbit polyclonal antibody against chorein (NBP1-85641; Novus Biologicals, Littleton, CO, USA) overnight at 4 °C. After washing with PBS-T, the sperm were incubated with secondary antibodies (Alexa Fluor

555 Goat Anti-Rabbit IgG (H+L), Invitrogen) for 1 h at room temperature. Coverslips were washed, mounted with Vectashield medium containing DAPI (Vector Laboratories, Burlingame, CA, USA), and viewed with a BZ-X 710 fluorescence microscope system (Keyence) using a sectioning technique.

2.7. Measurement of sperm adenosine 5'-triphosphate (ATP) concentration

The ATP concentration was measured using an ATP bioluminescent assay kit (Sigma-Aldrich, St. Louis, USA) according to the manufacturer's instructions.

2.8. Electron-microscopy analysis

Sperm were fixed with equal amounts of 4% paraformaldehyde (PFA) and 4% glutaraldehyde (GA) in 0.1 M cacodylate buffer pH 7.4 at incubation temperature, then refrigerated to lower their temperature to 4 °C. Thereafter, they were fixed with 2% GA in 0.1 M cacodylate buffer pH 7.4 at 4 °C overnight. After fixation, the samples were washed three times with 0.1 M cacodylate buffer for 20 min each, and were post-fixed with 2% osmium tetroxide (OsO4) in 0.1 M cacodylate buffer at 4 °C for 2 h. The

samples were dehydrated in graded ethanol solutions (50% ,70%, 90%, 100%). The schedule was as follows: 50% and 70% for 20 min each at 4 °C, 90% for 20 min at room temperature, and four changes of 100% for 20 min each at room temperature. The samples were infiltrated with propylene oxide (PO) twice for 20 min each, and then put into a 70:30 mixture of PO and resin (Quetol-812; Nisshin EM Co., Tokyo, Japan) for l h. The cap of the tube was then left open and the PO was volatilized overnight. The samples were transferred to fresh 100% resin, and were polymerized at 60 °C for 48 h. The polymerized resins were ultra-thin sectioned at 70 nm with a diamond knife using an ultra-microtome (Ultracut UCT; Leica, Vienna, Austria), and the sections were mounted on copper grids. These were stained with 2% uranyl acetate at room temperature for 15 min, and then washed with distilled water, followed by secondary-staining with lead-stain solution (Sigma- Aldrich Co., Tokyo, Japan) at room temperature for 3 min. The grids were observed with a transmission electron microscope (JEM-1400Plus; JEOL Ltd., Tokyo, Japan) at an acceleration voltage of 100 kV. Digital images (3296 × 2472 pixels) were taken with a CCD camera (EM-14830RUBY2; JEOL Ltd., Tokyo, Japan).

2.9. Statistical analysis

All statistical analyses were performed using Welch's t-tests for comparisons between wild-type and $ChAc^{Del/Del}$ mice. All data are shown as mean ± standard deviation (SD) for normally distributed continuous variables. $P < 0.05$ was considered to indicate a statistically significant difference.

3. Results

3.1. Confirmation of male infertility in ChAc-model mice

To confirm male infertility in ChAc-model mice, we housed each male $ChAc^{Del/Del}$ mouse with each of the female wild-types for at least 15 weeks. None of these females became pregnant. Conversely, all female $ChAc^{Del/Del}$ mice that were mated with male wild-types did become pregnant. In addition, in the sexual behavior test, no pregnancy was observed when male $ChAc^{Del/Del}$ mice were mated with female wild-types (Fig. 1C).

3.2. Sexual ability, sperm count, and sperm motility

Generally, male infertility is caused by lower sexual ability or problems with sperm production or motility. To investigate sexual ability, we performed an odor-sniffing test and sexual behavior test. In the odor-sniffing test, male $ChAc^{Del/Del}$ mice displayed increased investigation times for cotton swabs soaked with female urine. This increased investigation time was comparable to male wild-types (Fig. 1A). Each of the male mice was paired with a female mouse and their behavior was recorded for 1 h during the dark phase, and the total number of mountings by the male was scored (Fig. 1B). There was no significant difference in the number of mountings between $ChAc^{Del/Del}$ and wild-type mice. After the mating behavior test, a 66.7% pregnancy rate was observed in the female wild-types that had been paired with male wild-types. In contrast, no pregnancy was observed in female wild-types that had been paired with male $ChAc^{Del/Del}$ mice (Fig. 1C).

The number of sperm and the sperm anomaly rate were counted for at least 200 sperm per replicate. Then the sperm concentration and anomaly rate per region were calculated. Under light-microscope observation, there was no significant difference

between $ChAc^{Del/Del}$ and wild-type mice in either the sperm number or anomaly rate (Fig. 1D, E) when sperm were collected by scraping-out from the epididymis. However, the number of sperm obtained from the $ChAc^{Del/Del}$ mice was substantially lower than that obtained from the wild-types when the sperm were collected using the swim-up method (data not shown). Figure 1F shows the motility-failure rate of the sperm. A significantly higher rate was observed for the $ChAc^{Del/Del}$ mice, meaning that their sperm had significantly diminished motility.

3.3. Immunocytochemical study and ATP concentration levels

Chorein deficit induces severely reduced sperm motility. We therefore performed an immunofluorescence study to investigate chorein localization in the sperm. This revealed a chorein immunoreaction mainly in the midpiece of the sperm, which is a mitochondria-rich region (Fig. 2A). Since MitoTracker Green FM appears to localize to mitochondria regardless of mitochondrial membrane potential, we used MitoTracker red cationic fluorophores, for assessing the mitochondrial membrane potential in $ChAc^{Del/Del}$ mice sperm, and found that the mutant sperm stained normally (Fig. 2B).

We subsequently investigated the ATP production ability of these sperm, but found no significant differences in ATP concentration levels between $ChAc^{Del/Del}$ and wild-type sperm.

3.4. Electron-microscopy analysis

Our transmission electron microscopy analysis revealed that in the midpiece region of wild-type sperm, mitochondria were arranged spirally around the axon to form a mitochondrial sheath. In contrast, in $ChAc^{Del/Del}$ sperm, the mitochondria displayed marked variability in their size and an irregular sequence, and there were lower densities in the matrix and membrane (Fig. 2D). No marked differences in the head, tail, or axon structures were observed between the $ChAc^{Del/Del}$ and wild-type sperm.

4. Discussion

Loss of chorein leads to male infertility in mice; however, the reproductive ability of human male ChAc patients is generally intact. Indeed, in our own clinical experience, a human male ChAc patient who was a proband in a previously reported ChAc pedigree

(Case 3 in Family C in Ueno et al. [2]) with a *VPS13A* exon 60–61 deletion mutation had two children. Generally, male infertility is caused by decreased sexual behavior or sperm abnormality. In the present study, to investigate sexual behavior, we performed odor-sniffing and mating-behavior tests. In the odor-sniffing test, $ChAc^{Del/Del}$ mice displayed attraction to the smell of female urine comparable to male wild-types (Fig. 1A). In a previous study, $ChAc^{Del/Del}$ mice showed decreased learning ability [6]. Our $ChAc^{Del/Del}$ mice displayed a longer search time when investigating the male-odor stimulus than wild-type mice, which might reflect cognitive dysfunction. The mating-behavior test also revealed that the male $ChAc^{Del/Del}$ mice had retained sexual behavior (Fig. 1B).

In the present study, the sperm motility test revealed that the loss of chorein results in asthenozoospermia. In the sperm count test, there was no significant difference in the number of sperm when sperm were collected by scraping-out from the epididymis (Fig. 1D). However, the number of $ChAc^{Del/Del}$ sperm was substantially lower than that of wild-type sperm when the sperm were collected using the swim-up method (data not

shown). This probably reflects a decrease in sperm motility, which was also revealed by the subsequent sperm motility test.

Immunofluorescence revealed that chorein was localized in the mitochondria-rich midpiece of the sperm cell (Fig. 2A). Electron microscopy revealed that loss of chorein resulted in morphological abnormalities in mitochondrial sheaths in the midpiece, although light microscopy did not reveal morphological differences between $ChAc^{Del/Del}$ and wild-type sperm. These results suggest that loss of chorein leads to mitochondrial dysfunction. However, preserved ATP production ability and mitochondrial membrane potential (Fig. 2B, C) were observed in the loss-of-chorein sperm.

Sperm motility is manifested by proper function of the axoneme, which comprises microtubules and ATP-dependent dynein motors. There are unresolved arguments regarding ATP production and utilization in mammalian sperm motility. Although ATP is thought to be mainly provided by oxidative phosphorylation in the mitochondria, glycolytic activity is also required in the flagellum of mouse sperm [13]. Together with our results, these findings suggest that something other than the disturbance of mitochondrial respiration, which is related to the ultrastructural disturbances of

mitochondrial morphology caused by chorein deficit, is responsible for midpiece-related sperm motility defects. However, this unknown mechanism may play a different role in human sperm motility because human male patients with ChAc generally have reproduction ability.

Aparicio et al. reported that proteins related to autophagy/mitophagy processes were present in sperm and were possibly associated with the regulation of aspects of sperm function such as motility and viability [14]. Interestingly, Sasaki et al. reported that chorein was possibly involved in the clearance of subcellular organelles via autophagy to starvation-induced cell death resistance, which may involve chorein interactions with α-tubulin and HDAC6 [15]. In addition, Park et al. reported that yeast VPS13 localized to the membrane contact site was important for mitochondrial integrity, and suppressed the mitophagy pathway [16].

Considering our results and the above discussion, the following hypothesis may be made: loss of chorein may cause disruption of the autophagy/mitophagy pathway, resulting in disruptions of sperm mitochondrial integrity, ultrastructural morphological abnormalities in sperm mitochondria, and impairments of sperm motility in mice.

Although further analyses are needed to identify in molecular detail the motility defect that is related to midpiece mitochondria, these results suggest that chorein plays important roles in maintaining ultrastructural mitochondrial morphology and ATP-independent motility function in mouse sperm.

Conflict of Interest

The authors declare no conflict of interest.

Acknowledgments

The authors thank Ms. Hiwatashi, Ms. Yokoyama and Ms. Meguro for her technical assistance. We also thank Ms. Gohara and Mr. Yamashita for sperm count and analyzing video records of odor sniffing test and mating behavior test. We thank all staff members of the Institute of Laboratory Animal Sciences, Kagoshima University (Frontier Science Research Center) who kept the animals in good condition. This work was supported by Grants-in Aid from the Research Committee of CNS Degenerative Diseases, Research on Policy Planning and Evaluation for Rare and Intractable Diseases, Health, Labour and Welfare Sciences Research Grants, the Ministry of Health, Labour and Welfare, Japan, and in part by a Grant-in-Aid for Scientific

Research from the Ministry of Education, Culture, Sports, Science and Technology of Japan (No. 17H04250 to A.S. and No. 18K07606 to M.N.).

References

[1] L. Rampoldi, C. Dobson-Stone, J.P. Rubio, A. Danek, R.M. Chalmers, N.W. Wood, et al. A conserved sorting-associated protein is mutant in chorea-acanthocytosis, Nat. Genet. 28 (2001) 119–120. doi:10.1038/88821.

[2] S. Ueno, Y. Maruki, M. Nakamura, Y. Tomemori, K. Kamae, H. Tanabe, et al. The gene encoding a newly discovered protein, chorein, is mutated in chorea-acanthocytosis, Nat. Genet. 28 (2001) 121–122. doi:10.1038/88825.

[3] C. Dobson-Stone, A. Velayos-Baeza, L.A. Filippone, S. Westbury, A. Storch, T. Erdmann, et al. Chorein detection for the diagnosis of chorea-acanthocytosis, Ann. Neurol. 56 (2004) 299–302. doi:10.1002/ana.20200.

[4] A. Tomiyasu, M. Nakamura, M. Ichiba, S. Ueno, S. Saiki, M. Morimoto, et al. Novel pathogenic mutations and copy number variations in the *VPS13A* gene in

patients with chorea-acanthocytosis, Am. J. Med. Genet. B Neuropsychiatr. Genet. 156B (2011) 620–631. doi:10.1002/ajmg.b.31206.

[5] Y. Tomemori, M. Ichiba, A. Kusumoto, E. Mizuno, D. Sato, S. Muroya, et al. A gene-targeted mouse model for chorea-acanthocytosis, J. Neurochem. 92 (2005) 759–766. doi:10.1111/j.1471-4159.2004.02924.x.

[6] H. Sakimoto, M. Nakamura, O. Nagata, I. Yokoyama, A. Sano. Phenotypic abnormalities in a chorea-acanthocytosis mouse model are modulated by strain background, Biochem. Biophys. Res Commun. 472 (2016) 118–124. doi:10.1016/j.bbrc.2016.02.077.

[7] M. Nakamura, Y. Katoh, K. Yutaka, Y. Kurano, M. Ichiba, M. Matsuda, et al. A mouse model of chorea-acanthocytosis, in: Neuroacanthocytosis Syndromes II, Springer Berlin Heidelberg (2008) pp. 153–159. doi:10.1007/978-3-540-71693-8_12.

[8] A. Gil-Nagel, L. Morlán, J. Balseiro, J. García de Yébenes, A. Cabello, et al. Neuro-acanthocytosis with associated myopathy: a case report, Neurología 9 (1994) 165–168.

[9] Y. Kurano, M. Nakamura, M. Ichiba, M. Matsuda, E. Mizuno, M. Kato, et al. In vivo distribution and localization of chorein, Biochem. Biophys. Res. Commun. 353 (2007) 431–435. doi:10.1016/j.bbrc.2006.12.059.

[10] K. Kobayakawa, R. Kobayakawa, H. Matsumoto, Y. Oka, T. Imai, M. Ikawa, et al. Innate versus learned odour processing in the mouse olfactory bulb, Nature 450 (2007) 503–508. doi:10.1038/nature06281.

[11] S. Haga, T. Hattori, T. Sato, K. Sato, S. Matsuda, R. Kobayakawa, et al. The male mouse pheromone ESP1 enhances female sexual receptive behaviour through a specific vomeronasal receptor, Nature 466 (2010) 118–122.

doi:10.1038/nature09142.

[12] World Health Organization. WHO Laboratory Manual for the Examination and Processing of Human Semen, Fifth Edition (2010).

[13] S.S. du Plessis, A. Agarwal, G. Mohanty, M. van der Linde. Oxidative phosphorylation versus glycolysis: what fuel do spermatozoa use? Asian J. Androl. 17 (2015) 230–235. doi:10.4103/1008-682X.135123.

[14] I.M. Aparicio, J. Espino, I. Bejarano, A. Gallardo-Soler, M.L. Campo, G.M. Salido, et al. Autophagy-related proteins are functionally active in human spermatozoa and may be involved in the regulation of cell survival and motility, Sci. Rep. 6 (2016) 33647. doi:10.1038/srep33647.

[15] N. Sasaki, M. Nakamura, A. Kodama, Y. Urata, N. Shiokawa, T. Hayashi, et al. Chorein interacts with α-tubulin and histone deacetylase 6, and overexpression

preserves cell viability during nutrient deprivation in human embryonic kidney 293 cells, Faseb. J. 30 (2016) 3726–3732. doi:10.1096/fj.201500191RR.

[16] J.-S. Park, M.K. Thorsness, R. Policastro, L.L. McGoldrick, N.M. Hollingsworth, P.E. Thorsness, et al. Yeast Vps13 promotes mitochondrial function and is localized at membrane contact sites, Mol. Biol. Cell. 27 (2016) 2435–2449. doi:10.1091/mbc.E16-02-0112.

Figure legends

Fig. 1. Sexual behavior, sperm counts, sperm anomaly rates, and sperm motility in ChAc$^{Del/Del}$ mice. (A) An odor-sniffing test was performed. Statistically, no significant difference was observed in the duration of investigation of female urine by male ChAc$^{Del/Del}$ and wild-type mice. The investigation time for the third presentation of male urine was significantly longer for the mutants ($*p < 0.05$). (B) Sexual behaviors of ChAc$^{Del/Del}$ and wild-type males with wild-type females were observed and the number of male mountings was counted. No significant difference was observed between ChAc$^{Del/Del}$ and wild-type males. (C) After the sexual-behavior tests, a 66.7% pregnancy rate was observed in females mated with wild-type males, but no pregnancy was observed in females mated with ChAc$^{Del/Del}$ males. (D) There was no significant difference in the number of sperm scraped off from the epididymides. (E) Sperm anomaly rates did not differ between ChAc$^{Del/Del}$ and wild-type mice. (F) A significantly higher motility-failure rate was observed in ChAc$^{Del/Del}$ sperm than in wild-type sperm ($*** p < 0.001$). Data presented are means ± SD.

Fig. 2. Chorein localized to the mitochondria-rich midpiece of the sperm, and ultrastructural morphological abnormalities in the mitochondria were observed in the midpiece of ChAc$^{Del/Del}$ mouse sperm. (A) Sperm cells from ChAc$^{Del/Del}$ and wild-type mice were stained with Mitotracker Green FM (green) and anti-chorein antibody (red). Sperm nuclei were visualized with DAPI staining. Scale bars: 20 μm. (B) Sperm cells from ChAc$^{Del/Del}$ and wild-type mice were stained with Mitotracker Red. Scale bars: 20 μm. (C) There was no significant difference in the ATP concentration of ChAc$^{Del/Del}$ and wild-type sperm. (D) Transmission electron microscopy was performed for sperm from ChAc$^{Del/Del}$ and wild-type mice. Longitudinal and cross sections of the sperm midpiece were examined for mitochondrial ultrastructural anomalies. Dysmorphic mitochondrial structures were observed in ChAc $^{Del/Del}$ sperm. Scale bars for the longitudinal sections and cross sections are 20 μm and 1 μm, respectively.

Figure 1

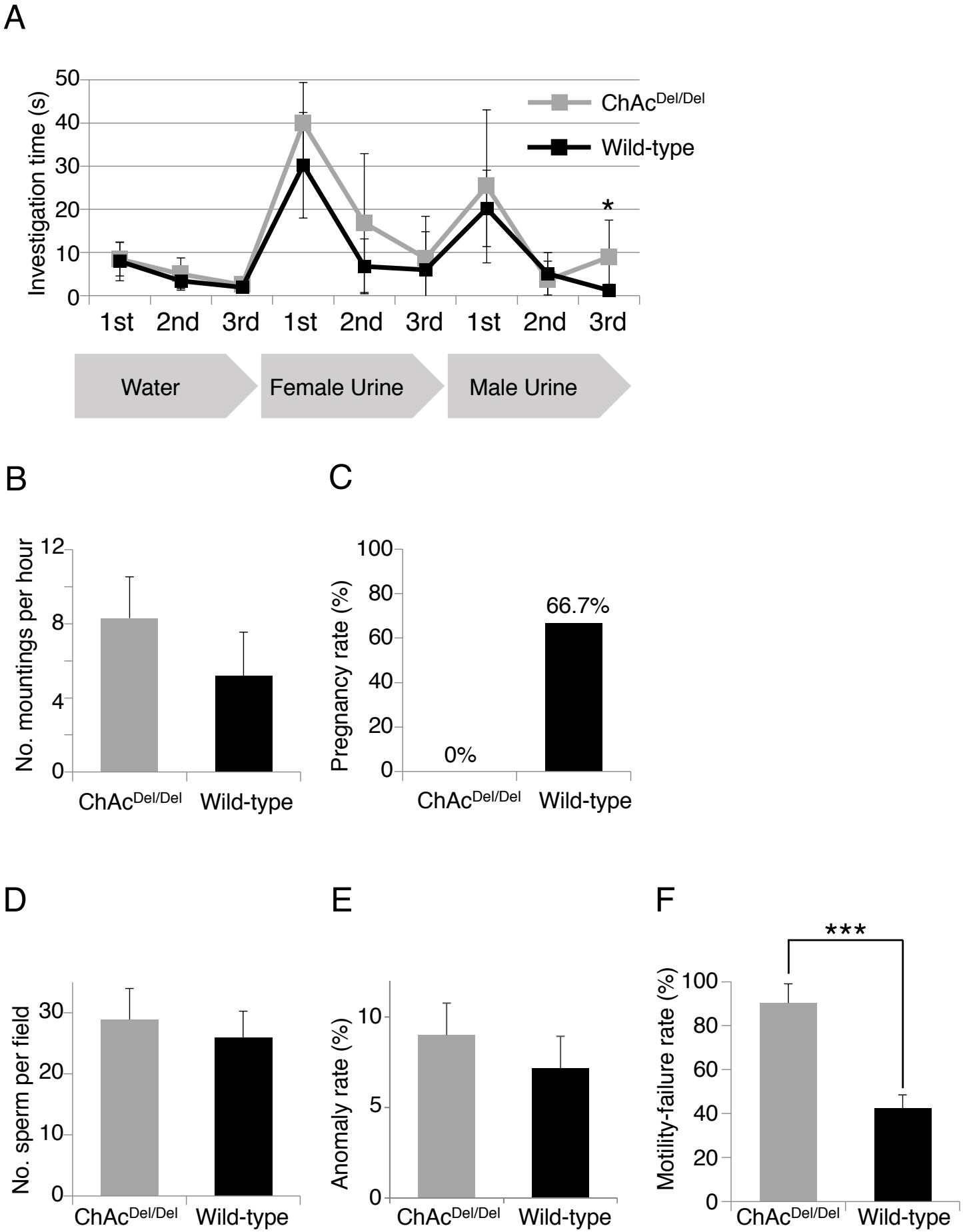
A
Investigation time (s)
50
40
30
20
10
0
ChAcDel/Del
Wild-type
*
1st
2nd
3rd
1st
2nd
3rd
1st
2nd
3rd
Water
Female Urine
Male Urine
B
No. mountings per hour
12
8
4
0
ChAcDel/Del
Wild-type
C
Pregnancy rate (%)
100
80
60
40
20
0
66.7%
0%
ChAcDel/Del
Wild-type
D
No. sperm per field
30
20
10
0
ChAcDel/Del
Wild-type
E
Anomaly rate (%)
10
5
0
ChAcDel/Del
Wild-type
F
***
Motility-failure rate (%)
100
80
60
40
20
0
ChAcDel/Del
Wild-type

Figure 2

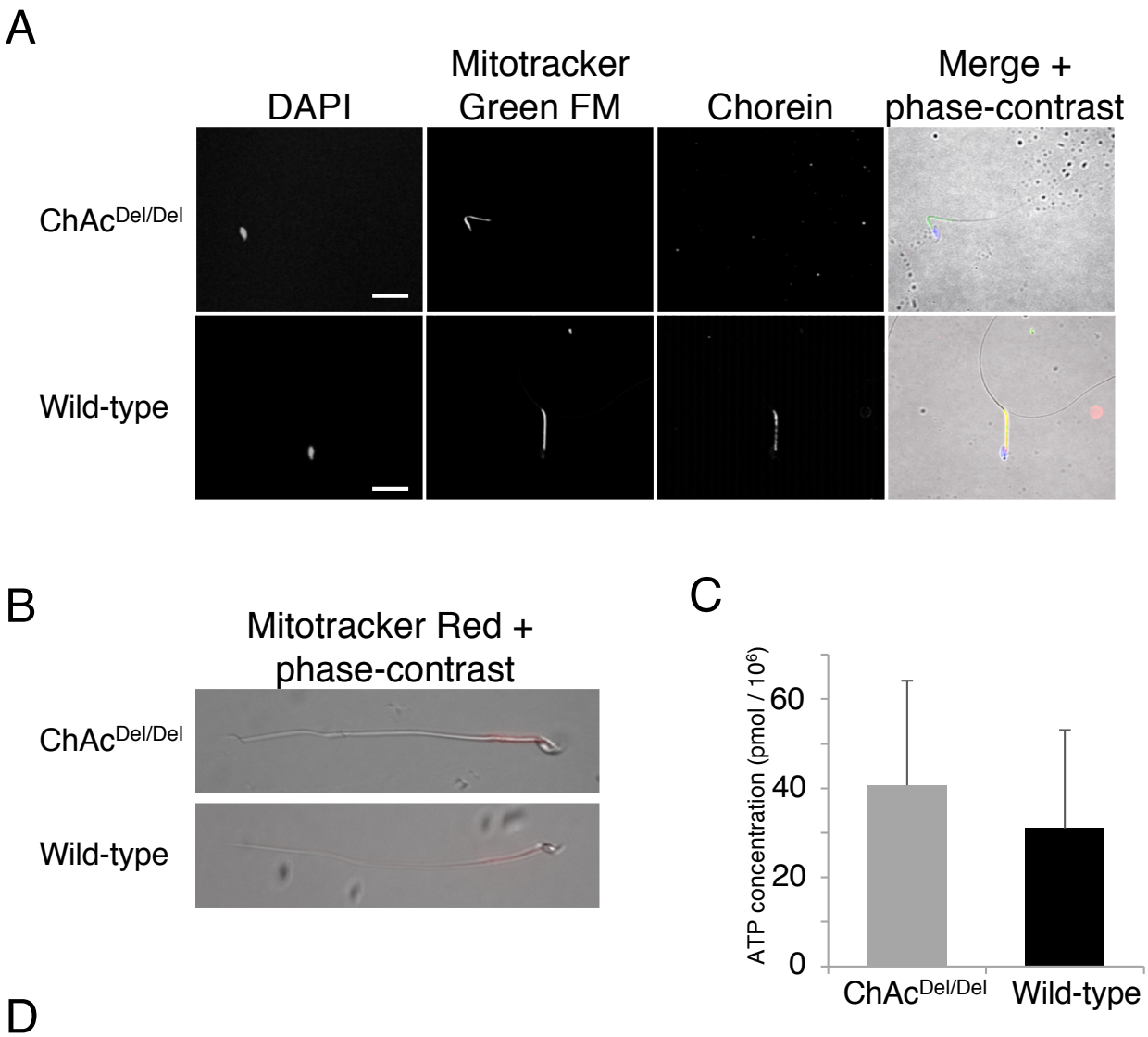
A
DAPI
Mitotracker Green FM
Chorein
Merge + phase-contrast
ChAcDel/Del
Wild-type
B
Mitotracker Red + phase-contrast
ChAcDel/Del
Wild-type
C
ATP concentration (pmol / 10^6)
60
40
20
0
ChAcDel/Del
Wild-type
D
ChAcDel/Del
Wild-type